

The Influence of As-Built Surface Conditions on Mechanical Properties of Ti-6Al-4V Additively Manufactured by Selective Electron Beam Melting

Y.Y. SUN,¹ S. GULIZIA,² C.H. OH,² D. FRASER,² M. LEARY,¹
Y.F. YANG,¹ and M. QIAN^{1,3}

1.—School of Aerospace, Mechanical and Manufacturing Engineering, Centre for Additive Manufacturing, RMIT University, Melbourne, VIC 3000, Australia. 2.—Commonwealth Scientific and Industrial Research Organisation (CSIRO), Manufacturing Flagship, Clayton, Melbourne, VIC 3168, Australia. 3.—e-mail: ma.qian@rmit.edu.au

Achieving a high surface finish is a major challenge for most current metal additive manufacturing processes. We report the first quantitative study of the influence of as-built surface conditions on the tensile properties of Ti-6Al-4V produced by selective electron beam melting (SEBM) in order to better understand the SEBM process. Tensile ductility was doubled along with noticeable improvements in tensile strengths after surface modification of the SEBM-fabricated Ti-6Al-4V by chemical etching. The fracture surfaces of tensile specimens with different surface conditions were characterised and correlated with the tensile properties obtained. The removal of a 650- μm -thick surface layer by chemical etching was shown to be necessary to eliminate the detrimental influence of surface defects on mechanical properties. The experimental results and analyses underline the necessity to modify the surfaces of SEBM-fabricated components for structural applications, particularly for those components which contain complex internal concave and convex surfaces and channels.

INTRODUCTION

Selective electron beam melting (SEBM) is a powder-bed-based additive manufacturing (AM) process, which is well suited to the manufacturing of titanium (Ti) materials due to the high-vacuum building chamber involved. Ti-6Al-4V (wt.%) is the benchmark Ti material and also the most studied metallic alloy for AM. To date, SEBM has found important applications in the commercial production of Ti-6Al-4V implants,^{1–3} while its applications in other industrial sectors are quickly emerging.⁴ Despite these encouraging developments, the understanding of the performance of SEBM-fabricated Ti-6Al-4V is still at an early stage. One less understood influence is that of the surface conditions. As with other powder-bed-based AM processes, the surfaces of SEBM-fabricated Ti parts suffer from two generic issues, (1) the partially melted Ti powder particles (the particles used for SEBM are usually much coarser than those used for

selective laser melting, SLM), and (2) the stair-case effect arising from the mismatch between the computer-aided design model and slicing strategy. As a result, SEBM-fabricated Ti parts often have a rough surface (e.g. $R_a = 30\text{--}68\ \mu\text{m}$ compared to $R_a < 1\ \mu\text{m}$ for machined surfaces).^{5,6} Although the detrimental influence of surface roughness on the mechanical properties of a metallic alloy is generally known, there is no quantitative understanding for Ti-6Al-4V, and in fact it is not an important issue in the context of traditional manufacturing. However, for additively manufactured Ti-6Al-4V and other metallic alloys, it is clearly an important issue. First, many innovative designs for AM contain intricate internal structures including micro-channels (<1 mm in diameter) and small diameter macro-channels (>1 mm in diameter), thin walls (<2 mm) and complex concave and convex surfaces. In most cases, the finish of an external surface is manageable by a variety of methods, but it is difficult to do the same for many interior surfaces.

To what extent will the imperfections of these interior surfaces discount the mechanical properties? In particular, Ti-6Al-4V produced by either SEBM⁷ or SLM⁸ shows a full-columnar structure along the building direction. There are surface flaws which are parallel to the columnar direction but there are also surface flaws which are perpendicular to the columnar direction. The latter type of flaws can be more detrimental than the former type. This stands out as an important concern from a design perspective, especially when the SEBM-fabricated part is designed for structural applications. A detailed literature survey has found only one related study, which showed that the fatigue properties of Ti-6Al-4V samples, produced by direct metal laser sintering and SEBM, are dominated by surface roughness effects.⁹ Second, surface roughness is also known to exert an important influence on the fluid flow behavior in microtubes¹⁰ and small diameter tubes.¹¹ For SEBM-fabricated Ti-6Al-4V components which contain similar internal structures for fluid flow functions, can their inner surface roughness be effectively improved, e.g. by acid etching? Third, for either the external or internal surfaces of Ti-6Al-4V produced under typical SEBM conditions, it is informative to know from a design perspective the approximate amount of surface layer thickness that should be removed in order to eliminate the negative influence of the surface flaws. This is especially the case for the design of thin-walled internal structures. Motivated by these questions, the purpose of this study is threefold: (1) to quantitatively identify the influence of surface conditions on the tensile properties of SEBM-fabricated Ti-6Al-4V; (2) to assess the effectiveness of acid etching in improving the surface finish of SEBM-fabricated Ti-6Al-4V; and (3) to produce first-hand experimental data for the design of Ti-6Al-4V by SEBM from a surface finish management perspective.

EXPERIMENTAL METHODS

Materials and Manufacturing

Extra low interstitial (ELI) gas atomized Ti-6Al-4V powder (ASTM Grade 23, 0.10 wt.% O, 0.01 wt.% N, 0.03 wt.% C, 0.1 wt.% Fe, <0.003 wt.% H) with a particle size range of 45–106 μm ($D_{50} = 73.52 \mu\text{m}$) was used. Nine tensile specimens (ASTM 1391-1991, 25 mm gauge length, $\Phi 10$ mm in grip section and $\Phi 5$ mm in gauge section) were manufactured vertically on a stainless steel base plate (200 mm \times 200 mm) in one batch without support using an Arcam A1 system. The processing parameters are summarized in Table I.

Surface Modification

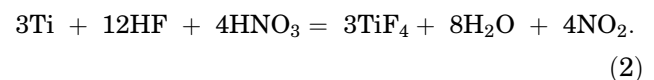
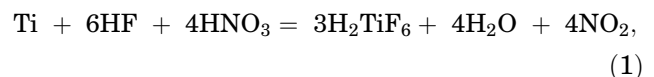
Both chemical etching and machining were used in this research to modify the surfaces of SEBM-fabricated Ti-6Al-4V specimens. The selection of

Table I. SEBM parameters used for fabrication

Parameters	Values
Software version	3.2.121
Acceleration voltage	60 kV
Beam current	1–10 mA
Beam spot size	200 μm
Speed factor	98
Scanning line offset	0.1 mm
Focus offset	5 mA
Layer thickness	50 μm
Preheating temperature	730°C
Vacuum	2.0×10^{-3} mbar

chemical etching is based on the following considerations. As pointed out earlier, the finish of an external surface can be modified by a variety of methods including machining, laser polishing,¹² electrical discharge machining,¹³ shot peening,¹⁴ shape adaptive grinding,¹⁵ burnishing¹⁶ and laser re-melting.¹⁷ However, none of them is suited to modifying the surfaces of internal structures in an intricate part. Chemical etching appears to be the only practical option in this regard.

Three tensile specimens were etched in Kroll reagent (3 mL 48% HF, 6 mL 70% HNO₃, 100 mL water, volume content of HF is 1.32%) at room temperature. Each specimen was placed vertically in a beaker with 250 mL fresh Kroll reagent and the following reactions are expected to occur:¹⁸



The mass of each specimen and its gauge diameter and surface roughness at the gauge section were measured every 30 min. The specimen was returned to the beaker upside down after each measurement in order to ensure uniform etching. The total etching time was 120 min. After that, all specimens were neutralized for 10 min in a dilute NaOH solution and rinsed thoroughly with tap water.

Characterization of Surface Conditions

A field emission scanning electron microscope (FESEM; Zeiss Merlin) and an Alicona infinite focus microscope (IFM; IF-EdgeMaster G4 Vb; Alicona Imaging, Graz, Austria) were used to visualize the surface morphology of the as-fabricated, surface-etched and machined specimens. An area of 2.04 mm \times 2.04 mm selected from the surface of the gauge section part was evaluated using the IFM. A conventional stylus-type profilometer (Perthometer S5P; Mahr, Germany) was used to quantify the

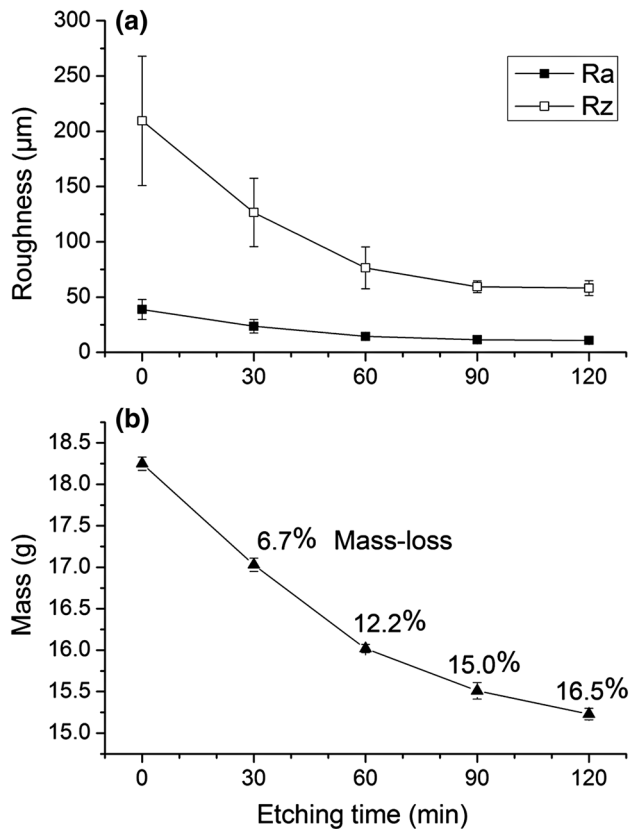


Fig. 1. Evolution of (a) surface roughness and (b) specimen mass as a function of etching time. The numbers in (b) indicate the mass loss.

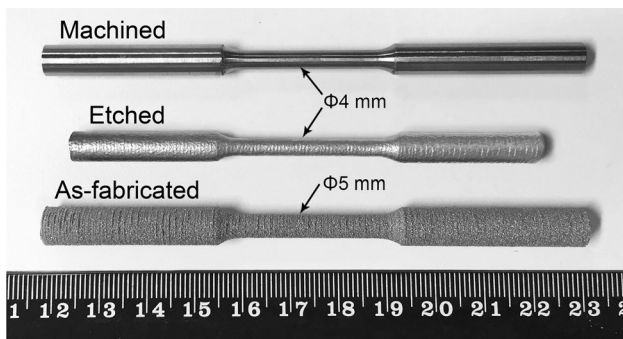


Fig. 2. Appearance of Ti-6Al-4V tensile specimens fabricated by SEBM: as-fabricated, surface-etched, and machined.

surface roughness of the gauge section. The evaluation length was 12.5 mm along the building direction. The surface roughness parameters R_a and R_z (R_z is the mean peak-to-valley height) were calculated from the surface profiles according to the ASME B46.1-2009.

Tensile Testing

Tensile testing was performed on an Instron tester (Model 5569, 50 kN load cell; Instron, Norwood, MA, USA) at a crosshead speed 0.5 mm/min at room temperature. A 25-mm clip-on extensometer was

attached to the specimen for strain measurement. The diameter used for calculating the cross-section area is $D_{out} - 2R_z$, where D_{out} is the outmost gauge diameter. The fracture surfaces were investigated using an FESEM.

RESULTS AND DISCUSSION

The evolution of surface roughness as a function of etching time is shown in Fig. 1a and the corresponding mass loss is shown in Fig. 1b. After 120 min etching, the R_a and R_z values were reduced from 38.9 μm to 10.9 μm (a reduction of 72%) and 209.5 μm to 58.19 μm (also a reduction of 72%), respectively. As a result, the surface roughness improved substantially. This is clear from comparing as-fabricated samples with surface-etched samples shown in Fig. 2. A noticeable mass loss was recorded (Fig. 1b). The improvement in surface roughness leveled out after 90 min etching, although the mass loss tends to continue.

Representative surface conditions of the as-fabricated, surface-etched and machined specimens are shown in Fig. 3, obtained using the FESEM (Fig. 3a–c) and the Alicona IFM (Fig. 3a'–c'). The as-fabricated surface contained a large number of partially melted particles (Fig. 3a and a'). Surface etching was successful to remove all these particles from the surface and smooth the surface, although it left a number of shallow dents on the surface (Fig. 3b and b'). The machined surface (Fig. 3c and c') showed the smoothest surface finish as measured by its R_a (0.13 μm) and R_z (0.95 μm) values.

Figure 4a compares the representative tensile stress–strain curves obtained from the as-fabricated, surface-etched and machined specimens. Each individual group of specimens exhibited consistent tensile responses, which are shown separately in Fig. 4b–d. Table II lists the average tensile properties together with their relative densities (the theoretical density is taken to be 4.43 g/cm³).¹⁹ The as-fabricated specimens are essentially pore-free (99.7% dense) and the relative density remained unchanged after surface etching or machining. Also listed in Table II are the minimum tensile properties and typical tensile properties of mill-annealed Ti-6Al-4V for comparison. The as-fabricated Ti-6Al-4V tensile specimens showed no obvious necking stage on their stress–strain curves (Fig. 4b) in contrast to the surface-etched and machined specimens (Fig. 4c and d). Their ultimate tensile strength (UTS) failed to meet the typical UTS of mill-annealed Ti-6Al-4V while their tensile elongation (5.75%) is more than 40% lower than the minimum tensile elongation (10%) required for mill-annealed Ti-6Al-4V. Etching the surface doubled the tensile elongation from 5.75% to 11.7%, along with a noticeable increase (~15%) in both the UTS and yield strength. Machining the surface led to very similar tensile elongation but slightly lower tensile strengths (~40 MPa lower) than did etching.

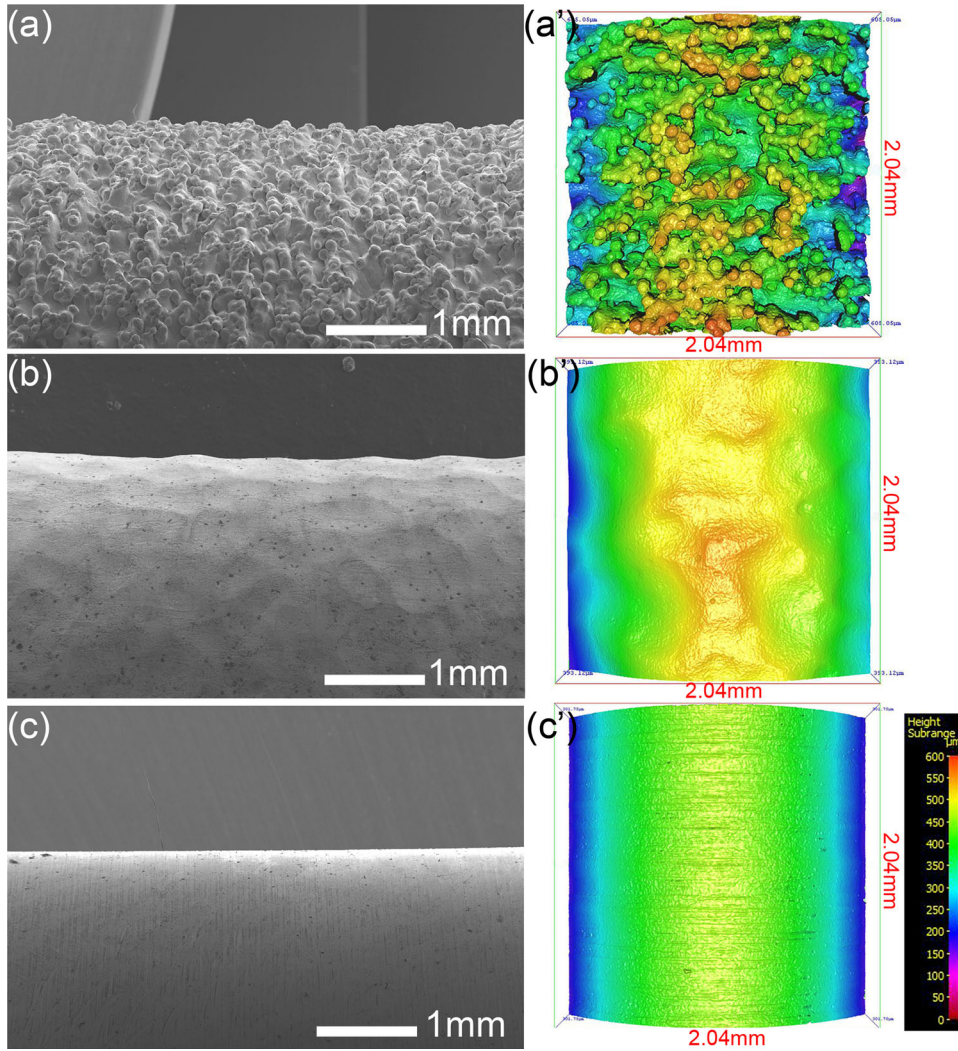


Fig. 3. (a), (b) and (c) are SEM surface images of as-fabricated, surface-etched and machined Ti-6Al-4V specimens, respectively, while (a'), (b') and (c') are respective surface conditions of as-fabricated, surface-etched and machined Ti-6Al-4V specimens observed under Alicona IFM, where the characterized area is 2.04 mm \times 2.04 mm.

These results indicate that the surface condition of the as-built Ti-6Al-4V specimens by SEBM has a significant influence on their mechanical properties and in fact it can be decisive.

Figure 5a–c show the macro tensile fracture surfaces of the as-fabricated, surface-etched and machined specimens while Fig. 5a'–c' are closer views of the boxed areas in (a), (b) and (c), respectively. The following observations are notable from the fracture surfaces.

As-fabricated (Fig. 5a and a') The fracture surface exhibited an incomplete cup-cone profile and a shear-lip free zone which spreads over about one-sixth of the periphery (marked by broken lines in Fig. 5a). A closer inspection of the shear-lip free zone (Fig. 5a'), revealed the existence of a number of defects in the surface layer including surface grooves and lack-of-fusion regions which are over 100 μm deep or wide. These large defects and the easy connections between them under tensile

loading led to straightforward fracture in this region from which cracks propagated to the rest of the specimen. The fracture surface showed a shear lip on the other side of the specimen at an angle of about 45° to the tensile stress axis, which is characteristic of ductile fracture. However, the shear lip stopped developing into the surface layer on the other side of the specimen, which is about 500 μm thick (see the broken line on the right-hand side of Fig. 5a). This surface layer defines the minimum thickness which needs to be removed from both the external and internal surfaces of an as-fabricated Ti-6Al-4V part for improved failure response.

Surface-etched (Fig. 5b and b') The fracture surface showed a typical cup-cone shape with a nearly continuous shear lip zone enveloping the central region of the specimen. Initial fracture started from a small shear-lip free region and propagated to the rest of the specimen (Fig. 5b). The shear-lip free

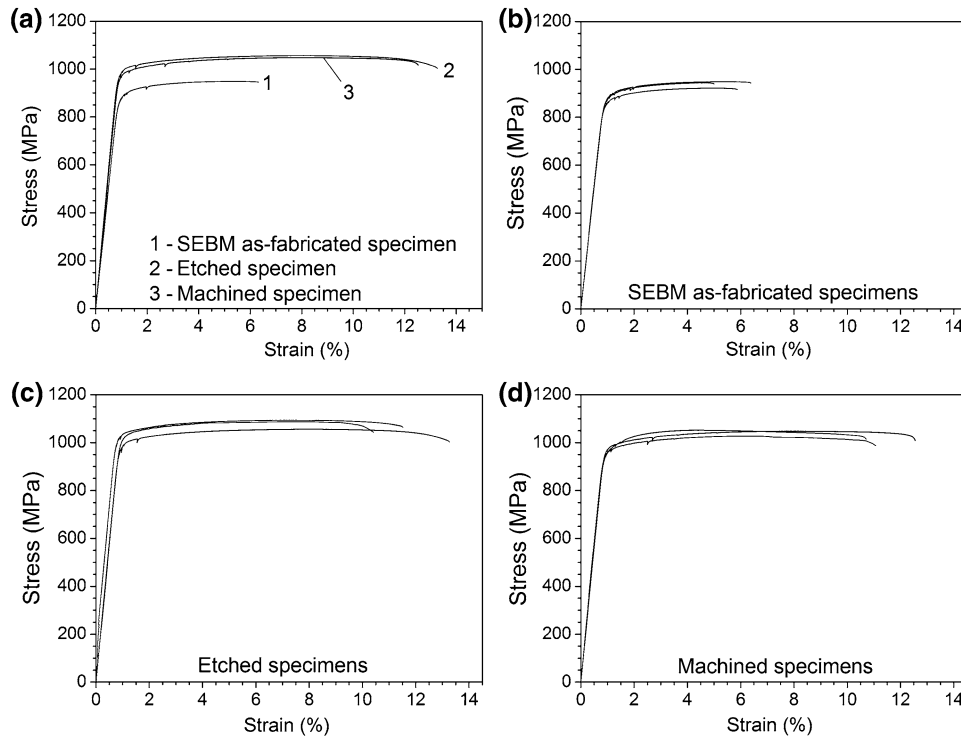


Fig. 4. Tensile stress–strain curves of as-fabricated, surface-etched and machined SEBM-fabricated Ti-6Al-4V. (a) Representative curves for each surface finish. Good consistency was observed in each case: (b) as-fabricated, (c) surface-etched, and (d) machined.

Table II. Tensile properties of SEBM-fabricated Ti-6Al-4V with different surface conditions

Specimens	Relative density (%TD)	$\sigma_{0.2}$ (MPa)	σ_{UTS} (MPa)	Elongation (%)
As-built	99.8 ± 0.1	878.8 ± 15.3	938.0 ± 14.2	5.75 ± 0.70
As-built + surface-etched	99.7 ± 0.3	1018.3 ± 25.9	1079.1 ± 19.9	11.7 ± 1.44
As-built + machined	99.8 ± 0.2	970.6 ± 8.7	1042.4 ± 12.9	11.4 ± 0.98
Mill-annealed (ASTM F136)	100	> 795	> 860	> 10
Mill-annealed (typical properties) ²⁰	100	875	965	13

$\sigma_{0.2}$ yield strength, σ_{UTS} ultimate tensile strength.

region, which is about 150 μm deep from the etched surface and 370 μm wide, still contained some lack-of-fusion defects (Fig. 5b'). The etching process removed a surface layer of about 500 μm thick from each tensile specimen. Figure 5b and b' indicates that a further removal of the surface up to 150 μm thick (650 μm in total) is necessary to eliminate the influence of major surface defects. For some fine internal structures in a complex SEBM-fabricated Ti-6Al-4V part such as a 1-mm-thick thin wall, this means that its section thickness will need to be increased by 1300 μm , making the design thickness to 2.3 mm in total. This can significantly change the original design. Limited necking occurred as shown by a thin bright ring along the periphery of the specimen. It has been reported that etching Ti in a

hydrofluoric acid solution may lead to the formation of a layer of titanium hydride^{21,22} which consequently could introduce hydrogen embrittlement. The as-etched Ti-6Al-4V specimen surfaces were analyzed using x-ray photoelectron spectroscopy (XPS). No trace of titanium hydride was detected.

Machined (Fig. 5c and c') The fracture surface is distinguished by a bright ring (300–600 μm thick) caused by necking during tensile testing and a nearly uniform continuous shear lip zone along the periphery. Unlike the fracture surfaces shown in Fig. 5a and b, the fracture appeared to have initiated from the interior defects in the specimen such as pores, which evolved into crater-like features on the fracture surface (Fig. 5c'). The complete removal of surface defects by machining resulted in

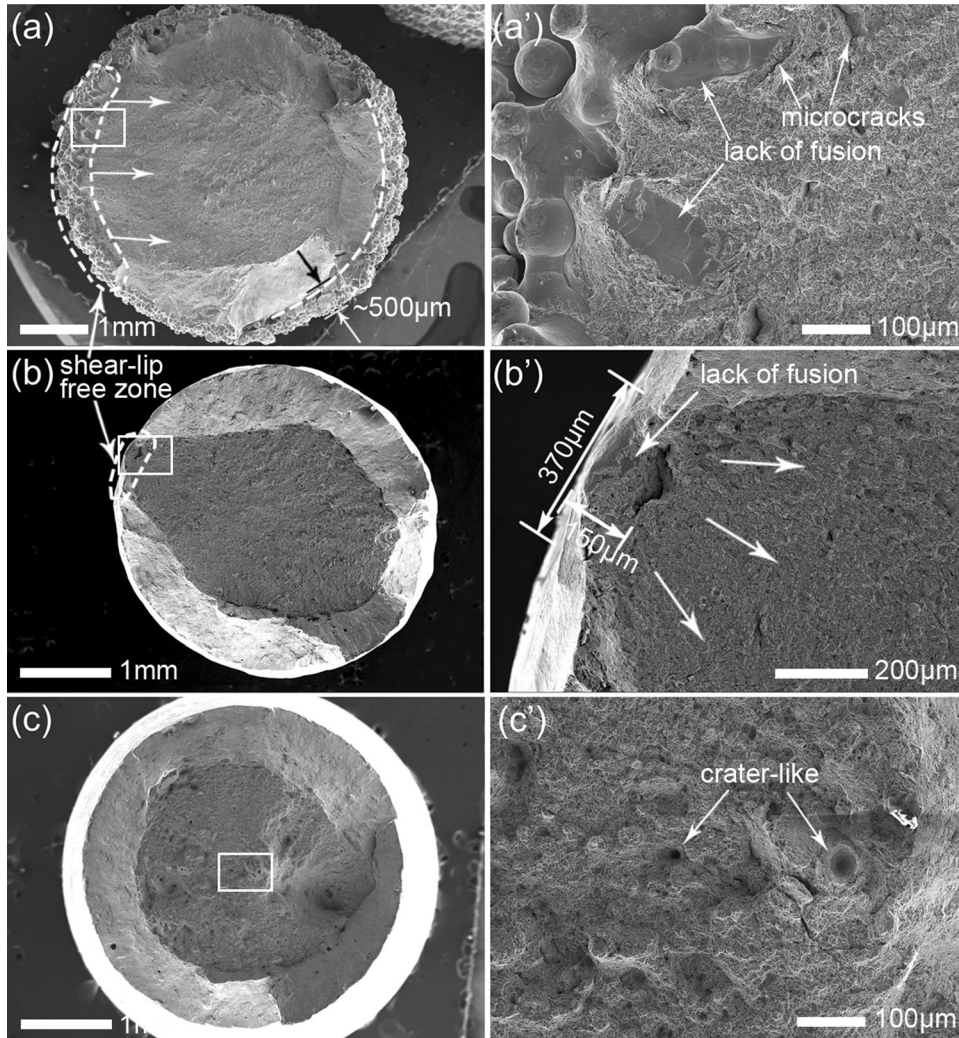


Fig. 5. Tensile fracture surfaces of SEBM-fabricated Ti-6Al-4V: (a) as-built; (b) surface-etched; (c) machined specimens. (a'), (b') and (c') are enlarged views of corresponding rectangle areas in (a), (b) and (c), respectively. The broken line areas in (a) and (b) indicate shear-lip free zones, where the cracks initiated. Arrows in (a) and (b') indicate crack propagation directions.

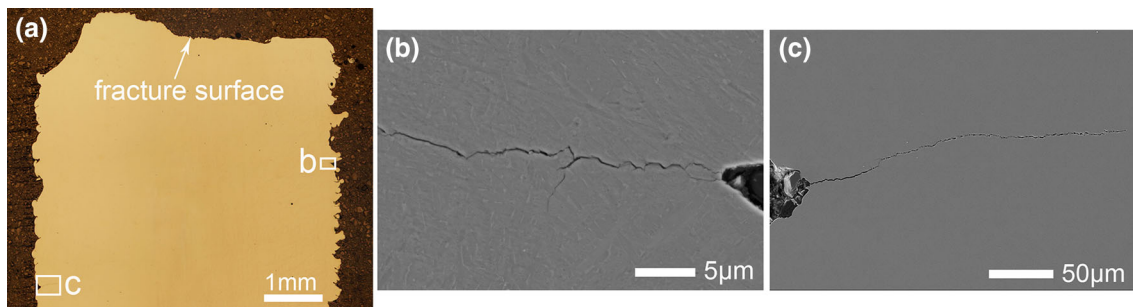


Fig. 6. (a) Optical image of a longitudinal section of an as-fabricated Ti-6Al-4V specimen by SEBM after tensile testing. (b) and (c) are SEM images showing microcracks observed in the boxed areas shown in (a).

distinctly different fracture characteristics. It is unfortunately impractical to machine many internal surfaces in an intricate part.

The central region of each fracture surface, i.e. the region enveloped by the shear-lip zone shown in Fig. 5, all showed similar dimples when inspected at

higher magnifications. This confirms that the difference in fracture behavior between the as-fabricated, surface-etched and machined samples is limited to their surface layers. To further reveal the influence of surface imperfections on crack initiation and propagation, a longitudinal section perpendicular to the fracture surface of an as-built tensile specimen was polished and shown in Fig. 6a. Five microcracks were observed to have initiated at the bottoms of respective surface grooves on this polished section. All these five surface grooves are perpendicular to the tensile loading direction. Figure 6b and c shows two such examples corresponding to the two boxed areas marked out in Fig. 6a. Surface grooves are high-stress concentration sites under tensile loading. They can lead to crack initiation or facilitate propagation of an existing crack at an accelerated speed under low applied tensile stresses, accounting for the much reduced tensile properties of the as-built specimens shown in Fig. 4. In contrast, no such microcracks were observed in surface-etched and machined specimens, further indicative of the effectiveness of surface modification.

It should be noted that, apart from the rough surface, the surface layer of SEBM-fabricated Ti-6Al-4V often contains pores of various sizes. Surface etching or machining has the effect of cleaning up both surface roughness and porosity at the same time. This positive secondary effect may also have contributed to the improved tensile properties. Regarding the influence of the as-built surface conditions on fatigue performance, a systematic study is still underway to assess this issue (uniaxial fatigue testing in ambient environment under 400 MPa, $R = 0.1$ and 10 Hz with fatigue specimens prepared according to ASTM E466-07, namely $\Phi 5$ mm test section, 20 mm test section length and 40 mm blending fillet radius). In the fatigue experiments performed to date, the number of cycles to failure of the as-built Ti-6Al-4V specimens at 400 MPa reached only about 2.0×10^4 , which increased to $\sim 8.0 \times 10^4$ after surface etching and further to $\sim 5.0 \times 10^5$ after machining. These preliminary results indicate that the fatigue performance is more sensitive to surface conditions than the tensile properties for SEBM-fabricated Ti-6Al-4V. Detailed experimental results will be reported in the near future including the additional influence of hot isostatic pressing.

SUMMARY

The influence of surface conditions on the tensile properties of SEBM-fabricated Ti-6Al-4V has been investigated. The surface finish can be decisive in determining the performance of SEBM-fabricated Ti-6Al-4V. Without surface modification, the as-fabricated Ti-6Al-4V specimens showed tensile elongation (5.75%) far below the minimum tensile elongation (10%) required for mill-annealed Ti-6Al-4V, and also low ultimate tensile strength (UTS)

and yield strength. Chemical etching using Kroll reagent doubled the tensile elongation and increased both the UTS and yield strength by 15% due to the much improved surface finish (the surface roughness was reduced from $38.9 \mu\text{m}$ to $10.9 \mu\text{m}$), making the surface-etched Ti-6Al-4V specimens comparable to machined specimens. The fracture of as-fabricated Ti-6Al-4V tensile specimens started from surface imperfections, leading to the formation of shear-lip free zones on the fracture surfaces. The removal of a $650\text{-}\mu\text{m}$ -thick surface layer by chemical etching is necessary to eliminate the detrimental influence of surface defects on mechanical properties based on the characterization of the fracture surfaces. This could be challenging for SEBM-fabricated intricate parts which contain fine internal structures. In this regard, it is important to continue to improve the AM process for better surface finish or the mechanical properties of the as-fabricated Ti-6Al-4V components should be discounted accordingly in considering their applications.

ACKNOWLEDGEMENTS

Y.Y. Sun acknowledges the support of the China Scholarship Council (CSC) for a CSC scholarship. M. Qian acknowledges the support of the Australian Research Council (ARC) through the Discovery Project Grant of DP150104719. Useful discussions with Prof. H.P. Tang, Director of the State Key Laboratory of Porous Metal Materials, Northwest Institute for Nonferrous Metal Research, Xi'an, China, are acknowledged.

REFERENCES

1. G. Chahine, M. Koike, T. Okabe, P. Smith, and R. Kovacevic, *JOM* 60, 50 (2008).
2. O.L. Harrysson, O. Cansizoglu, D.J. Marcellin-Little, D.R. Cormier, and H.A. West, *Mater. Sci. Eng., C* 28, 366 (2008).
3. L.E. Murr, S.M. Gaytan, E. Martinez, F. Medina, and R.B. Wicker, *Int. J. Biomater.* 2012, 245727 (2012).
4. S. Gaytan, L.E. Murr, F. Medina, E. Martinez, L. Martinez, and R.B. Wicker, *TMS 139th Annual Meeting & Exhibition*, vol. 1, 2010, pp. 283–290.
5. M. Jamshidinia and R. Kovacevic, *Surf. Topog. Met. Prop.* 3, 014003 (2015).
6. C.M. Haslauer, J.C. Springer, O.L. Harrysson, E.G. Lobo, N.A. Monteiro-Riviere, and D.J. Marcellin-Little, *Med. Eng. Phys.* 32, 645 (2010).
7. H. Tang, S. Lu, W. Jia, G. Yang, and M. Qian, *Int. J. Powder Metall.* 50, 57 (2014).
8. W. Xu, M. Brandt, S. Sun, J. Elambasseril, Q. Liu, K. Latham, K. Xia, and M. Qian, *Acta Mater.* 85, 74 (2015).
9. D. Greitemeier, C. Dalledonne, F. Syassen, J. Eufinger, and T. Melz, *Mater. Sci. Technol.* (2015). doi:10.1179/1743284715Y.0000000053.
10. G.M. Mala and D. Li, *Int. J. Heat Fluid Flow* 20, 142 (1999).
11. S.G. Kandlikar, S. Joshi, and S. Tian, *Heat Trans. Eng.* 24, 4 (2003).
12. I. Mingareev, T. Bonhoff, A.F. El-Sherif, W. Meiners, I. Kelbassa, T. Biermann, and M. Richardson, *J. Laser Appl.* 25, 052009 (2013).
13. K.S. Chan, M. Koike, R.L. Mason, and T. Okabe, *Metall. Mater. Trans. A* 44, 1010 (2013).
14. P. Edwards, A. O'Conner, and M. Ramulu, *J. Manuf. Sci. Eng.* 135, 061016 (2013).

15. A.T. Beaucamp, Y. Namba, P. Charlton, and A.A. Graziano, *ASPE Spring Meeting—Additive Manufacturing*, California, 2014.
16. Y. Bao, J. Newkirk, J. Ruan, T.E. Sparks, and F. Liou, *J. Manuf. Proc.* 10, 56 (2008).
17. E. Yasa, J. Deckers, T. Craeghs, M. Badrossamay, and J.P. Kruth, *International Solid Freeform Fabrication Symposium*, Austin, 2009.
18. J.W. Dini, *Am. Mach. Spec. Rep.* 768, 113 (1984).
19. ASME B46.1-2009: *Surface Texture (Roughness, Waviness and Lay)*.
20. M.J. Donachie, *Titanium: A Technical Guide*, 2nd ed. (Materials Park: ASM International, 2000).
21. S.F. Lamolle, M. Monjo, M. Rubert, H.J. Haugen, S.P. Lyngstadaas, and J.E. Ellingsen, *Biomaterials* 30, 736 (2009).
22. M.J. Frank, M.S. Walter, S.P. Lyngstadaas, E. Wintermantel, and H.J. Haugen, *Mater. Sci. Eng., C* 33, 1282 (2013).